Quest Journals
Journal of Research in Applied Mathematics
Volume 12 ~ Issue 4 (April 2026) pp: 01-21
ISSN (Online): 2394-0743 ISSN (Print): 2394-0735
www.questjournals.org

Research Paper

Fuzzy Graph Models and Machine Learning Approaches for Image Processing Applications

Dr. Adel Ahmed Hassan Kubba[1], Amal Abdallah Suliman Hamza[2]
Associate Professor- University of Nile Vally-Faculty of Education Department of Mathematics, adelkubba60@gmail.com, PhD student in mathematics at University of Nile Vally.

Abstract. *This paper presents fuzzy graph-based models integrated with machine learning techniques for analyzing topological indices and their applications in image processing tasks. The study focuses on ladder graphs and grid graphs and investigates both crisp and fuzzy topological indices including the First Zagreb Index, Second Zagreb Index, Randi Index, and Harmonic Index. Closed-form expressions for these indices are derived and analyzed. Linear regression models are applied to examine relationships between graph vertices and corresponding topological indices using machine learning tools. The results demonstrate strong linear correlations between graph order and topological measures. The study also introduces fuzzy ladder graphs and fuzzy grid graphs, extending classical graph measures into the fuzzy domain. Experimental analysis shows that fuzzy graph representations combined with machine learning regression improve interpretability and predictive capability in graph-based modeling. These models provide useful tools for applications such as image segmentation, network analysis, and computational pattern recognition.*

Keywords: *Fuzzy graphs, Ladder graph, Grid graph, Machine learning, Linear regression, Topological indices, Image processing.*

*Received 28 Mar., 2026; **R**evised 06 Apr., 2026; **A**ccepted 08 Apr., 2026 © The author(s) 2026.*
P**ublished with open access at **www.questjournals.org

I. Introduction

Graph theory and fuzzy systems play an important role in modeling complex systems with uncertainty. Fuzzy graph theory extends classical graph theory by allowing vertices and edges to have membership values in the interval [0,1]. This provides a powerful framework for representing uncertain relationships that frequently appear in real-world problems. Topological indices are numerical descriptors derived from graph structures and are widely used in chemistry, network analysis, and computational modeling. In recent years, the integration of machine learning techniques with graph theoretical models has attracted increasing attention. Machine learning algorithms enable the discovery of patterns and relationships between structural graph properties and numerical indices. In this work, ladder graphs and grid graphs are analyzed due to their regular structures and relevance in many practical systems such as transportation networks, electrical circuits, and image grids. Both crisp and fuzzy versions of these graphs are investigated. Linear regression models are applied to explore relationships between the number of vertices and several topological indices.

II. Methodology:

(2.1) [2] Molecular descriptor of ladder graph LG:

Ladder Graph (LG)can be obtained through the Cartesian product of path graph graph P_m and a path graph P_2 . The ladder graph is a Cartesian product of two graphs, denoted by$H_1 \times H_2$ has a vertex set $V(H_1 \times H_2) = V(H_1) \times V(H_2$ and every vertex of

$H_1 \times H_2$ is an ordered pair (x, y), where $x \in V(H_1) and y \in V(H_2)$. Two distinct vertices $(x_1, y_1)\ and\ (x_2, y_{2)}$ are adjacent in $H_1 \times H_2$

$if\ either\ x_1 = x_2\ \ and\ y_1y_2 \in E(H_2)$ or $y_1 = y_2\ \ and\ x_1x_2 \in E(H_1)$[98]

(2.1.1) Theorem: let $G = P_m \times P_2$ be a ladder graph, then the FZI of ladder graph $G = P_m \times P_2$ is $M_1(G) = (18m - 20)$, for $m \geq 2$.

Proof: The representation of ladder graph $G = P_5 \times P_2$ is in Fig.1. Ladder graph$G = P_m \times P_2$ having total 2m vertices out of which 4 vertices have degree 2 while the remaining 2m−4 have degree 3. The total number of edges of Ladder graph $G = P_m \times P_2$ are $3m - 2$.

$$\begin{aligned} M_1(G) &= \sum_{v \in V(G)} d^2(v) \\ &= 4[2^2] + (2m - 4)[3^2] \\ &= 16 + 18m - 36 \\ &= 18m - 20, \end{aligned}$$

(2.1.2) Theorem: Let $G = P_m \times P_2$ be a ladder graph,

1. then the SZI of the ladder graph is $M^*(G) = 27m - 40$, for $m \geq 2$.
2. then the RI of ladder graph is $R(G) = m - 0.027$, for $m \geq 2$.
3. then the HI of ladder graph is $H(G) = (m - 0.06)$, for $m \geq 2$.

Proof: part 1 The ladder graph $G = P_m \times P_2\ has\ 3m - 2$ edges consisting of three types of partitions for the edges are as follows:

The first partition of edges (2, 2) has 2 edges, degree of both end vertices is 2. the second partition of edges (2, 3) has 4 edges, one vertex has degree 2 and other vertex has degree 3, and third partition of edges (3, 3) has 3m−8 edges, degree of both end vertices is 3.

$$\begin{aligned} M^*(G) &= \sum_{jk \in E(G)} [d(j) \times d(k)] \\ &= 2[2 \times 2] + 4[2 \times 3] + (3m - 8)[3 \times 3] \\ &= 8 + 24 + 27m - 72 \\ &= 27m - 40, \end{aligned}$$

Proof: part 2**.** By using the same edge partition of Part 1. we have

$$\begin{aligned} R(G) &= \sum_{jk \in E(G)} [d(j) \times d(k)]^{-1/2} \\ &= [2][2 \times 2]^{-1/2} + [4][2 \times 3]^{-1/2} + [3m - 8][3 \times 3]^{-1/2} \\ &= 1 + 1.633 + m - 2.66 \\ &= m - 0.027, \end{aligned}$$

Proof: part 3**.** By using the same edge partition of Part 1. we have

$$\begin{aligned} H(G) &= \sum_{jk \in E(G)} \left[\frac{2}{d(j) + d(k)}\right] \\ &= \frac{2 \times 2}{2 + 2} + \frac{4 \times 2}{2 + 3} + \frac{2 \times (3m - 8)}{3 + 3} \\ &= 1 + \frac{8}{5} + \frac{3m - 8}{3} \\ &= 1 + 1.6 + m - 2.66 \\ &= m - 0.06, \end{aligned}$$

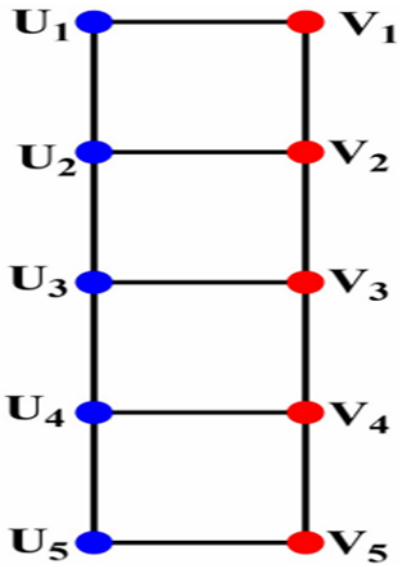

Figure (1.) Ladder graph $G = P_5 \times P_2$

After raising the values of m from 2 to 11 in the ladder graph $G = P_m \times P_2$ we get the values of different indices shown in Table1.

Ladder graph	1st Zagreb	2nd Zagreb	Randić	Harmonic
$P_2 \times P_2$	16	14	1.973	1.94
$P_3 \times P_2$	34	41	2.973	2.94
$P_4 \times P_2$	52	68	3.973	3.94
$P_5 \times P_2$	70	95	4.973	4.94
$P_6 \times P_2$	88	122	5.973	5.94
$P_7 \times P_2$	106	149	6.973	6.94
$P_8 \times P_2$	124	176	7.973	7.94
$P_9 \times P_2$	142	203	8.973	8.94
$P_{10} \times P_2$	160	230	9.973	9.94
$P_{11} \times P_2$	178	257	10.973	10.94

Table (1) Comparison of indices for $G = P_m \times P_2$ Ladder graph

(2.2) [2] Linear function derivation for ladder graphs via machine learning algorithms:

Machine learning (ML) plays a vital role in different areas, particularly in data-related daily life applications. ML s a branch of artificial intelligence analysis that focuses on building systems capable of learning from data to make predictions or decisions without being explicitly programmed. Among the various techniques in machine learning, regression analysis is widely used to model and analyze relationships with variables. Linear regression is a basic technique in ML. In linear regression, two variables are involved, one is independent and the other one is dependent. Linear regression builds a relationship between these variables to form a linear equation to observe the data. The equation of linear regression model is $y = \alpha_1 x + \alpha_0$ where y is the dependent variable, x is the independent variable, and $\alpha_{n,}\alpha_{n-1}, \ldots, \alpha_1 and\ \alpha_0$ are the corresponding coefficients.

Multi-linear regression with multiple independent variables along with a single dependent variable. The multi-linear regression equation is $y = \alpha_n x_n + \alpha_{n-1} x_{n-1} + \cdots . \alpha_1 x + \alpha_0$ where $\alpha_n, \alpha_{n-1}, \ldots . \alpha_1 \alpha_0$ are the coefficients of $x_n, x_{n-1}, \ldots . x_1$ respectively.

For this regression analysis, we will use Jupyter Notebook which is a very established server-client application that permits the code or editing in code. We will import our data after writing some code in a Jupyter Notebook. Afterward, we run our regression analysis code. The best-fit line equation is then obtained. We will also employ the coefficient of determination (R-squared), a statistical measure that will assist us in determining how near our data is to the best-fit line.

The regression analysis of the ladder graph between the vertices and FZI, SZI, RI, and HI. The equation of linear regression and their graph is presented in Table.2. below: First Zagreb Index The relationship between vertices and the FZI is represented by the equation and the graphical comparison shown in Fig..2a and b.

$$FZI = 9.0167 \times \text{Vertex} - 19.9778$$

Vertex	FZI	SZI	RI	HI
4	0.539	0.1414	18.2334	8.9419
6	0.86	0.2469	23.9089	11.7782
8	1.181	0.3524	29.5844	14.6144
10	1.502	0.4579	35.2599	17.4507
12	1.823	0.5634	40.9354	20.287
14	2.144	0.6689	46.6109	23.1232
16	2.465	0.7744	52.2864	25.9594
18	2.786	0.8799	57.9619	28.7957
20	3.107	0.9854	63.6374	31.6319

Table2. Table showing the relationship between Vertex, FZI, SZI, RI, and HI.

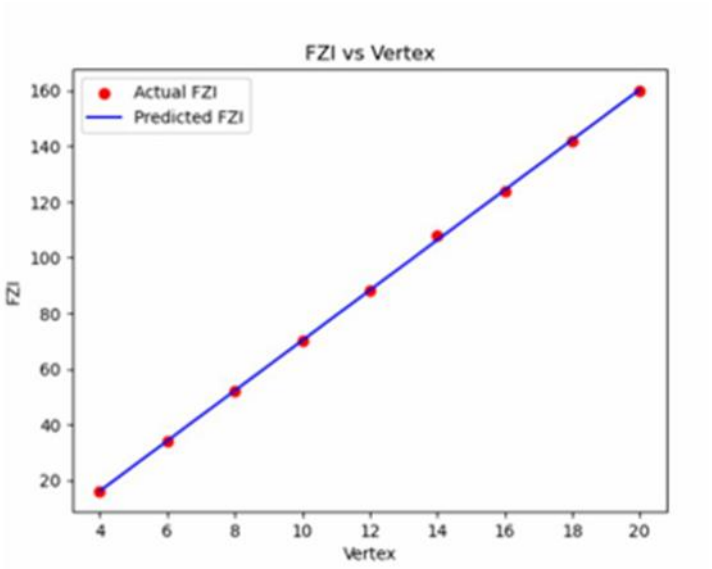

Figure 2a. First Zagreb index vs vertices. FZI vs vertices.

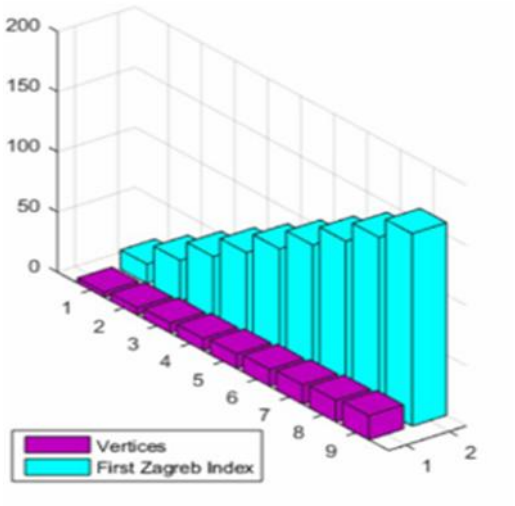

Figure2b. First Zagreb index vs vertices FZI Vs vertices. 3D plot.

(2.3) Zagreb indices of fuzzy ladder graph (FLG):

Second Zagreb Index The relationship between vertices and the SZI is represented by the equation and the graphical comparison shown in Fig.3a and b.

$$SZI = 13.5000 \times \text{ Vertex } - 40.0000$$

Randić Index The relationship between vertices and RI is represented by the equation and the graphical comparison shown in Fig 4a and b.

$$RI = 0.5000 \times \text{ Vertex } - 0.0270$$

Harmonic Index The relationship between vertices and HI is represented by the equation and the graphical comparison shown in Fig.5a and b.

$$HI = 0.5000 \times V\text{ertex } - 0.0600$$

(2.3.1) Theorem: Let $G = P_m \times P_2$ be a FLG, then the FFZI of the LG $G = P_m \times P_2$ *is* $FM_1(G) = (0.321m - 0.424) for\ m \geq 2$

Proof. All vertices $\acute{U}_i$s have weight 0.4 having total count m, in which m-2

having weight 0.7 while the remaining 2 have 0.4. All vertices $\acute{V}_i s$ have weight 0.5 having total count m, in which m-2 having weight 0.5 while the remaining 2 have 0.3.

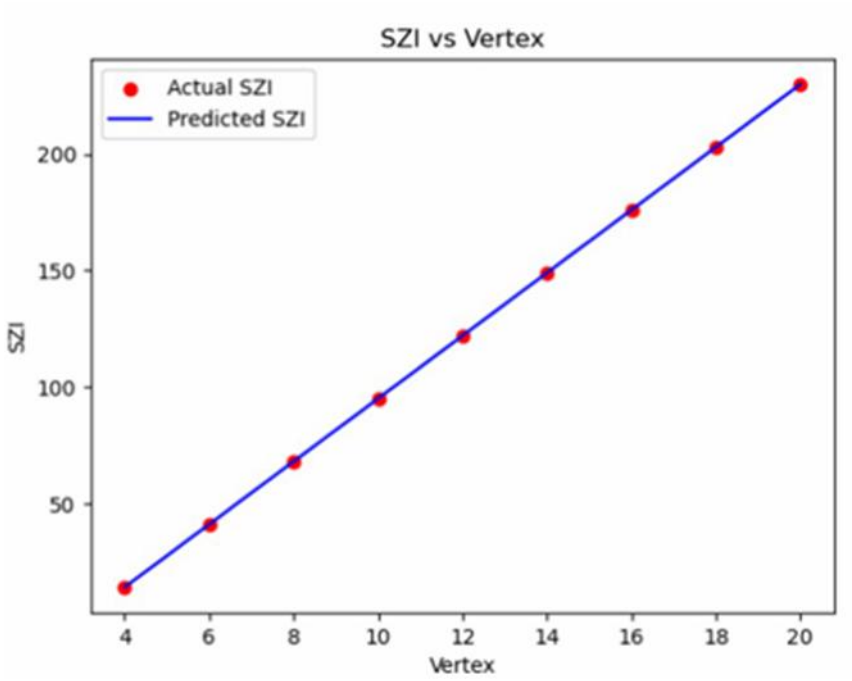

Figure.3a. Second Zagreb index vs vertices. SZI Vs Vertices.

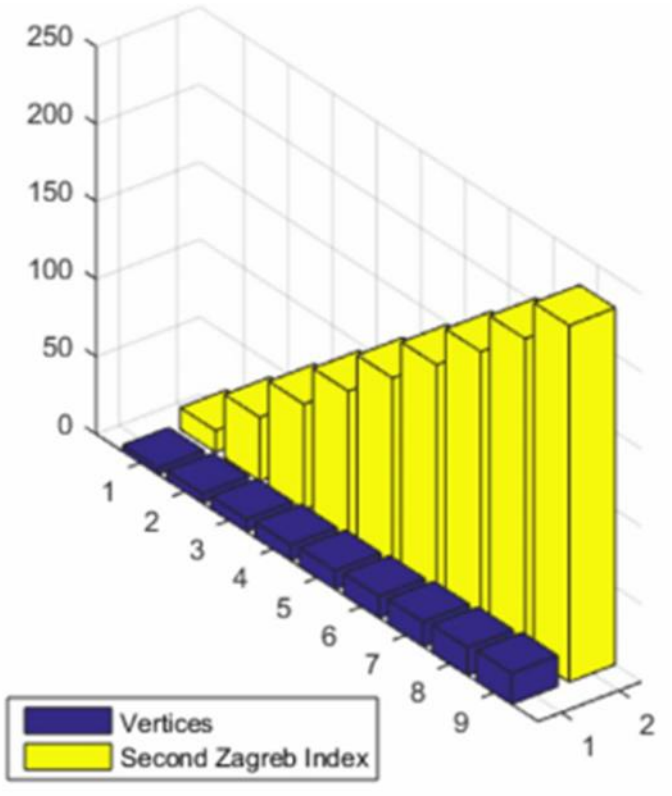

Figure.3b. Second Zagreb index vs vertices.3D plot.

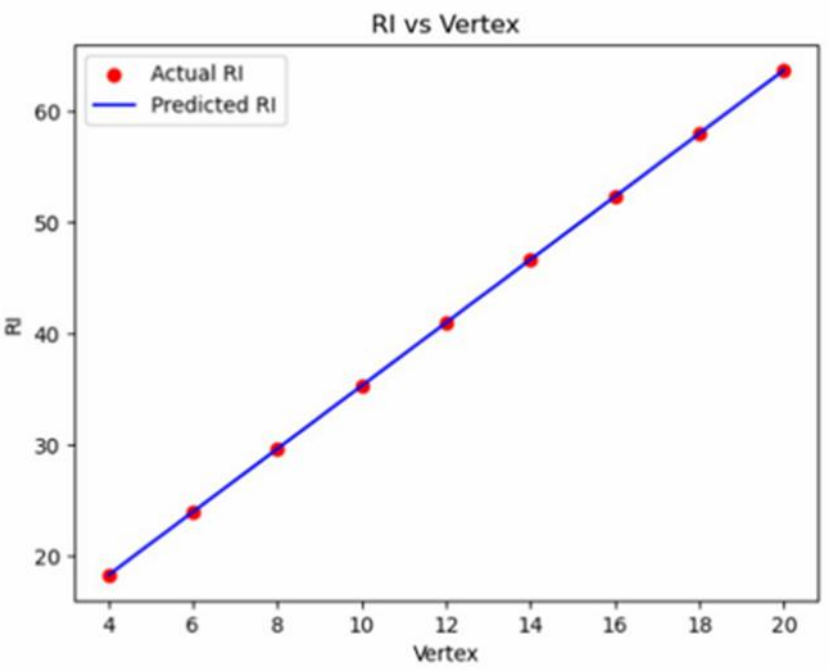

Figure.4a. Randić index vs vertices. RI Vs Vertices.

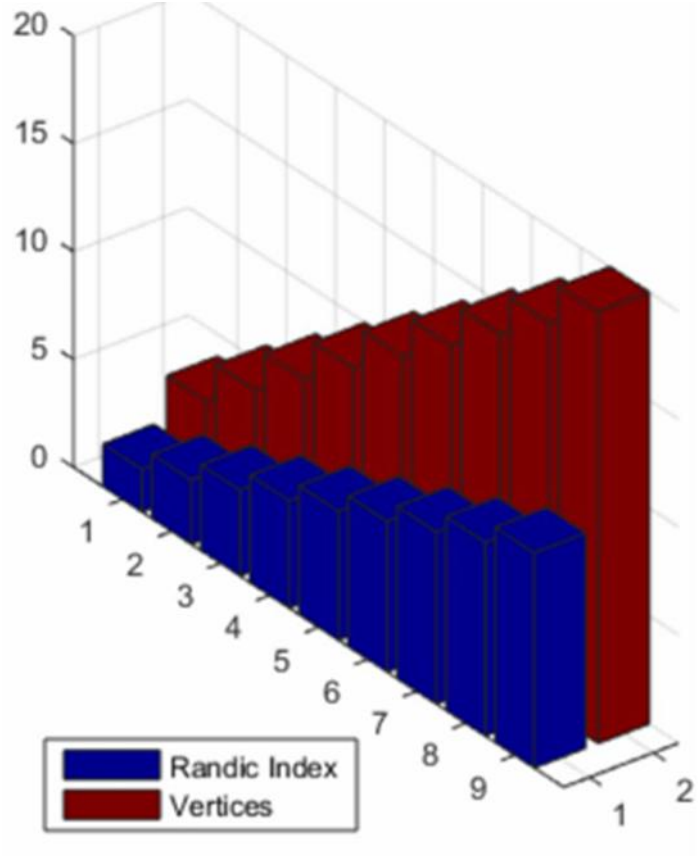

Figure.4b. Randić index vs vertices. RI Vs Vertices. 3D plot.

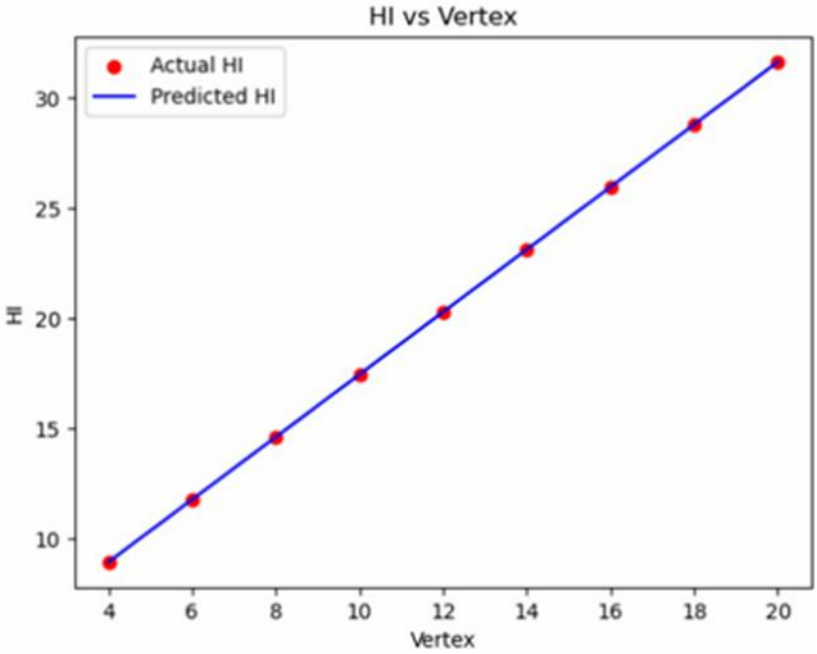

Figure. 5a. Randić index vs vertices. HI Vs Vertices.

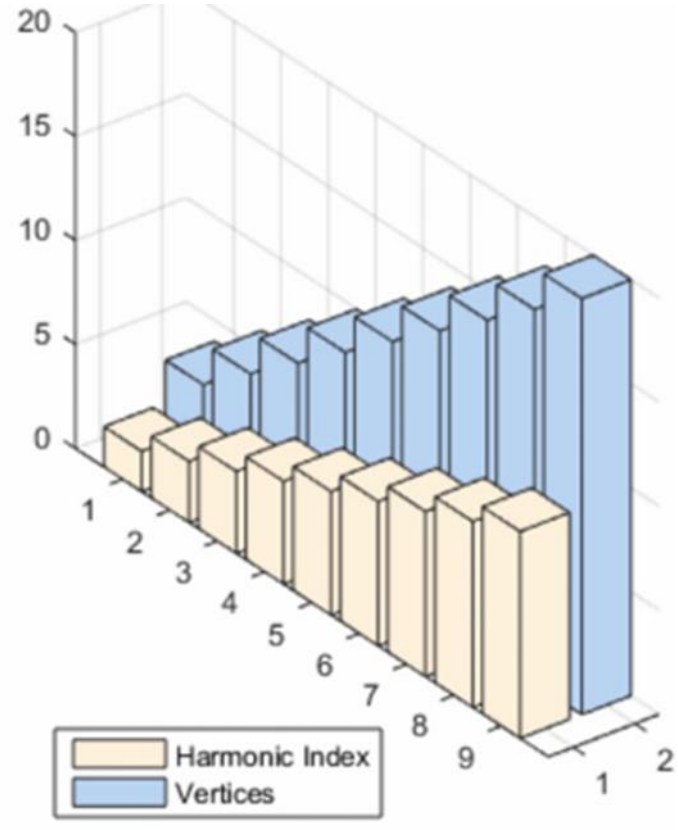

Figure. 5b. Randić index vs vertices. HI Vs Vertices. 3D plot

$$FM_1(G) = \sum_{k=1}^{q} \sigma(u_k)[du_k]^2,$$
$$= (0.4)[2(0.4)^2 + (m-2)(0.7)^2] + (0.5)[2(0.3)^2 + (m-2)(0.5)^2]$$
$$= (0.4)[0.32 + (m-2)(0.49)] + (0.5)[0.18 + (m-2)(0.25)]$$
$$= (0.4)[0.32 + 0.49m - 0.98] + (0.5)[0.18 + 0.25m - 0.50]$$
$$= 0.196m + 0.125m - 0.264 - 0.16$$
$$= 0.321m - 0.424,$$

Randić index, harmonic index, and fuzzy first and second Zagreb indices of grid graph have been discussed in this section. Grid graph can be obtained through the cartesian product of path P_m and P_n A Cartesian product of two graphs, denoted by $H_1 \times H_2$ has a vertex set$V(H_1 \times H_2) = V(H_1) \times V(H_2)$ and every vertex of $H_1 \times H_2$ is an ordered pair $(x,\ y)$, where $x \in V(H_1)$ and $y \in V(H_2)$.Two distinct vertices (x_1, y_1) $and (x_2, y_2)$ are adjacent in $H_1 \times H_2$ if either $x_1 = x_2$ and $y_1y_2 \in E(H_2)$ or $y_1 = y_2$ and $x_1x_2 \in E(H_1)$

(2.3.2)Theorem let $G = P_m \times P_n$ be a grid graph, then the first Zagreb index of grid graph $G = P_m \times P_n is$ $M_1(G) = (16mn - 14m - 14n + 8)$, for $m, n \geq 2$.

Proof. The representation of grid graph $G = P_m \times P_n$ having mn vertices and $2mn - (m + n)$ edges, is given below.

4 vertices have degree 2, $2(m + n - 4$ vertices have degree 3, while the remaining $mn - 2(m + n) + 4$ have 4.

$$M_1(G) = \sum_{v \in V(G)} d^2(v)$$
$$= 4[2^2] + 2(m + n - 4)[3^2] + (mn - 2(m + n) + 4)[4^2]$$
$$= 16mn - 14m - 14n + 8,$$

we will compute the fuzzy topological indices of the Fuzzy Grid Graph (FGG). We will use FGG for Fuzzy Grid Graph throughout this paper. The other notations will be used for fuzzy topological indices Such as the Fuzzy First Zagreb Index (FFZI), Fuzzy Second Zagreb Index (FSZI), Randić Index (RI), and Harmonic Index (HI). The total number of vertices of FGG is mn and the total edges are $2(m \times n) - (n + m)$

(2.2.3) Theorem let $G = P_m \times P_n$ be a FGG, then the FFZI is

$FM_1(0.108mn - 0.12n - 0.66m + 0.048), for\ m, n \geq 2$

Proof. The Weight of the all vertices $\acute{U}_i s$ is 0.3 and has a total count of $m \times n$

where 4 vertices have weight 0.3,$2(n - 2)$ vertices have weight 0.4, $2(n - 2)$ vertices have weight 0.5 and remaining $nm - (2m + 2m - 4)$ vertices have 0.6.

$$FM_1(G) = \sum_{k=1}^{q} \sigma(u_k)[du_k]^2,$$
$$= 0.3[4(0.3)^2 + 2(n-2)(0.4)^2$$
$$+2(m-2)(0.5)^2 + (mn - (2n + 2m - 4))(0.6)^2]$$
$$= (0.3)[0.36mn - 0.40n - 0.22m + 0.16]$$
$$= 0.108mn - 0.12n - 0.66m + 0.048,$$

(2.3) [15]A Fuzzy soft graph with applications in image segmentation:

In this section, we present a few important terms related to fuzzy set (FSs) and fuzzy graph (FGs).

(2.3.1) Definition A fuzzy set (FSs) F over a set $\check{V}$ is a mapping $\sigma_F: \check{V} \to [0,1]$, where $\sigma_F(\dot{u})$ represents the membership degree of $\dot{u}\ in\ F$.

(2.3.2) Definition A fuzzy graph (FG) defined on $\check{V}$ is the triplet $\tilde{G} = (\check{V}, \sigma, \varsigma)$, where $\sigma: \check{V} \to [0,1]$ and $\varsigma: \check{V} \times \check{V} \to [0,1]$ such that $\sigma(\dot{u}, \dot{v}) \leq \sigma(\dot{u}) \wedge \sigma(v)$, for all $u, v \in \check{V}$.

(2.3.3)Definition The degree of a vertex in a FMG $\dot{G} = (\breve{V}, \sigma, \breve{E})$ is defined as $d(\dot{u}) = \sum_{\dot{u}\in\vec{V}} \sum_{j=1}^{p_{\dot{u}\dot{v}}} (\dot{u}, \dot{v})_{\sigma^j}$. If a crisp graph contains at least one crossing between edges, then we call it a non-planar graph.

However, in an FG $G = (\breve{V}, \sigma, \varsigma)$, if there is a single crossing between two fuzzy edges $\big((x_1, y_1), \varsigma(x_1, y_1)\big)$ and $\big((x_2, y_2), \varsigma(x_2, y_2)\big)$ with $\varsigma(x_1, y_1) = 1$ and $\varsigma(x_2, y_2) = 0$, then we say $\tilde{G}$ has no crossing, for some particular geometric representation. Moreover, if $\varsigma(x_1, y_1)$ is close to 1 and $\varsigma(x_2, y_2)$ is close to 0, the crossing is not considerable. Alternatively, if both $\varsigma(x_1, y_1)$ and $\varsigma(x_2, y_2)$ are near 1,then the crossing effects the graph's planarity.

(2.3.4) Definition A fuzzy soft multi-graph (FSMG) $G^* = (\hat{G}, \hat{C}, \hat{Q}, A)$ can be defined as a 4-tuple, where

i. $\hat{G}$ represents a multi-graph consisting of vertices $\breve{V}$ and edges $\breve{E}$
ii. A denotes a non-empty subset of parameters
iii. $(\hat{C}, A)$ is a fuzzy soft multi-set (FSMS) defined on $\breve{V}$
iv. $(\hat{Q}, A)$ is a FSMS defined on $\breve{E}$, and for each parameter $c \in A$, the pair $(\hat{C}(c), \hat{Q}(c))$ forms a fuzzy (multi)graph of $\hat{G}$, satisfying the condition

$$\hat{Q}(u, v)_{\varsigma_c}(c) \leq min\{\hat{C}(u)(c), \hat{C}(v)(c)\}$$

for all $c \in A$ and $u, v \in \breve{V}$, where $(u, v)_{\varsigma cj}$ represents the membership value of $j - th$ fuzzy soft edge in FSMG $G^* \cdot \hat{H}(c)$ denotes the fuzzy multi-graph $(\hat{C}(c), \hat{Q}(c))$.

(2.3.5) Example Let $\hat{G} = (\breve{V}, \breve{E})$ be a multi-graph, where $\breve{V} = \{v_1, v_2, v_3, v_4\}$ and $\ddot{E} = \{v_1v_2, v_1v_4, v_1v_4, v_2v_3, v_2v_4, v_2v_4, v_3v_4, v_3v_4\}$. let $D = \{a_1, a_2, a_3, a_4, a_5\}$ be a collection of the set of parameters related to the above vertex set and $A = \{a_1, a_2, a_3\} \subset D$. Let $(\hat{C}, A)$ be FSMS defined over $\breve{V}$ such that $\hat{C}: A \to F(\breve{V})$ given by

$$\hat{C}(a_1) = \{v_1|0.8, v_2|0.2, v_3|0.0, v_4|0.5\}$$
$$\hat{C}(a_2) = \{v_1|0.2, v_2|0.8, v_3|0.6, v_4|0.4\}$$
$$\hat{C}(a_3) = \{v_1|0.8, v_2|0.7, v_3|0.3, v_4|0.5\}.$$

Let $(\hat{Q}, A)$ be FSMS defined over $\breve{E}$ such that $\hat{Q}: A \to F(\breve{E})$ given by

$$\hat{Q}(a_1) = \begin{Bmatrix} v_1v_2|0.3, v_1v_2|0.4, v_1v_4|0.5, v_2v_4| \\ 0.2, v_2v_4|0.6, v_1v_3|0.0, v_2v_3 \mid 0.0 \end{Bmatrix}$$
$$\hat{Q}(a_2) = \begin{Bmatrix} v_1v_2|0.0, v_1v_4|0.2, v_1v_4|0.1, v_2v_3| \\ 0.4, v_2v_4|0.1, v_2v_4|0.4, v_3v_4|0.2, v_3v_4|0.3 \end{Bmatrix}$$
$$\hat{Q}(a_3) = \begin{Bmatrix} v_1v_2|0.6, v_1v_2|0.7, v_2v_4|0.4, v_2v_4| \\ 0.1, v_2v_3|0.3, v_3v_4|0.2, v_3v_4 \mid 0.0 \end{Bmatrix}.$$

Then

$$\hat{H}(a_1) = \big(\hat{C}(a_1), \hat{Q}(a_1)\big)$$
$$\hat{H}(a_2) = \big(\hat{C}(a_2), \hat{Q}(a_2)\big)$$
$$\hat{H}(a_3) = \big(\hat{C}(a_3), \hat{Q}(a_3)\big)$$

are FMGs of $\hat{G}$ corresponding to parameters $a_1, a_2\ and\ a_3$ as shown in Fig.6. Consequently, the collection $G^* = (\hat{G}, \hat{C}, \hat{Q}, A)$ is a FSMG.

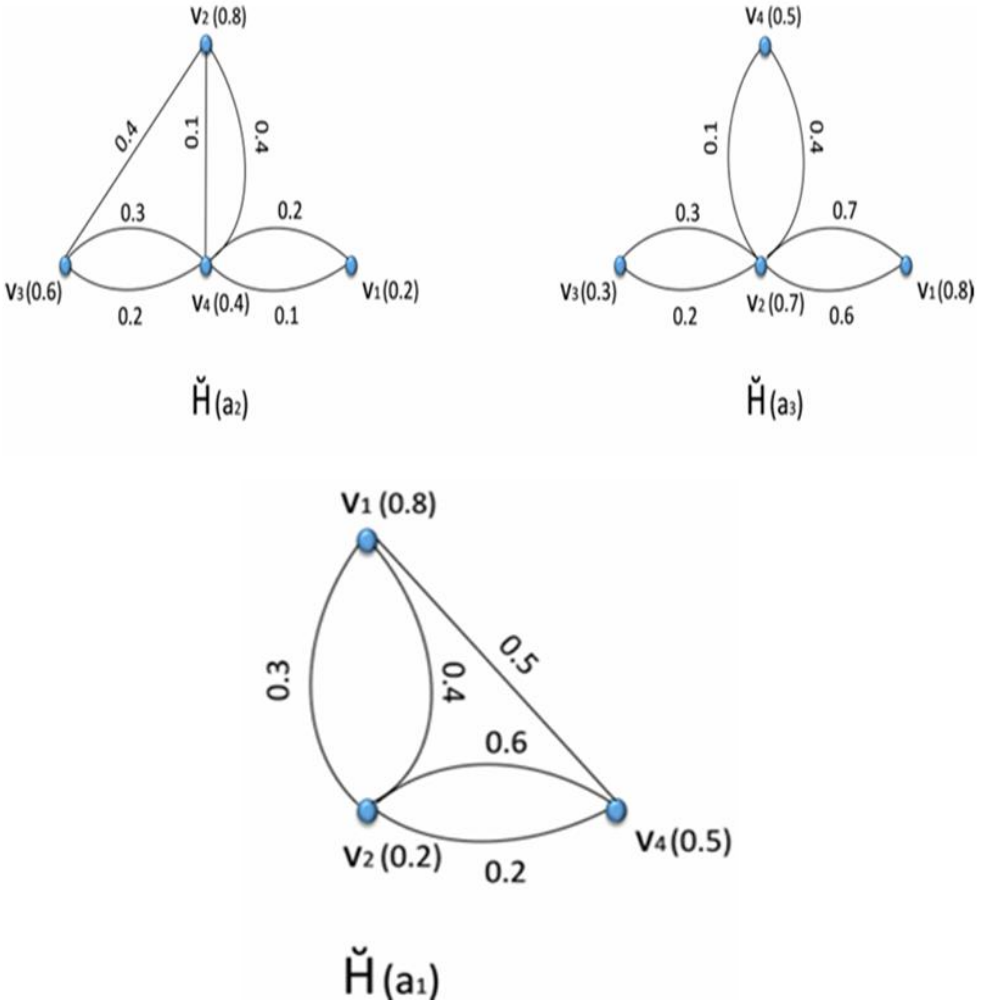

Fig.6. FSMG $\left(\hat{H}(a_1), \hat{H}(a_2), \hat{H}(a_3)\right)$

Image contraction based on fuzzy soft planar graphs (FSPGs). Image segmentation is a fundamental technique in digital image processing that partitions an image into distinct regions or objects. This process is crucial in various fields including image processing, MRI scanning and remote sensing as it helps to identify the objects of interest from the background in an image. In this section, we introduce a method for image segmentation based on fuzzy soft planar graphs (FSPGs). An image consists of pixels that form homogeneous regions which can be manipulated through appropriate planar graphs. Many researchers have been conducted in this field. However, the process of image segmentation/ contraction involves many uncertainties. Thus, FPGs are the best tool to handle uncertainties involved in such

Fig.7 An Asakusa Tokyo image. Left: original image. The next two segmented images are obtained by applying FSSs.

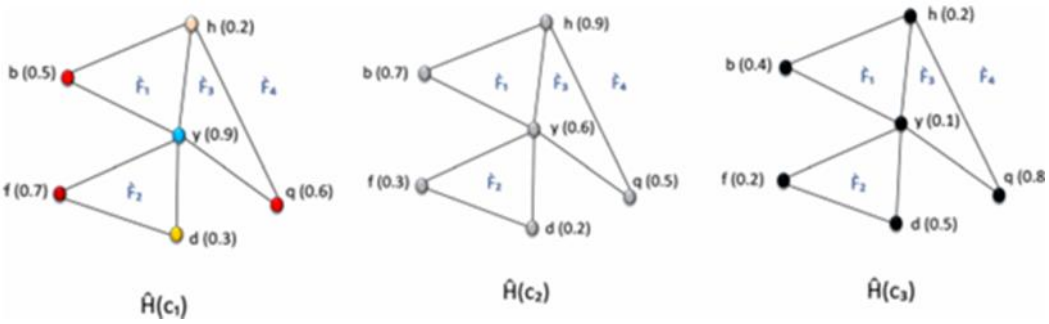

Fig.8. FSPG $G^* = \left(\hat{H}(c_1), \hat{H}(c_2), \hat{H}(c_3)\right)$ corresponding to fuzzy soft segmented image illustrated in Fig.7.

A process. Moreover, image processing has also been addressed through FPGs. Since FSPGs are the extended form of FGs, it would give us more precise results compared to FGs. Thus, we deal with the process of image segmentation through FSPGs. The key idea of our method is to deal images through FSG, where each pixel in the image serves as a fuzzy soft vertex in the graph. The membership value to each vertex (pixel) is allocated according to the intensity (or gray-scale value) of each pixel. Neighboring pixels (or vertices) are connected by fuzzy soft edges with their membership values determined by the intensity difference between the connected pixels. Several methods have been used to quantify pixel dissimilarity. However, in our model the membership value is lower for the higher dissimilarity and vice versa. In the next section, we first provide an algorithm for image segmentation contraction using FSPGs, and then apply it to an image of Asakusa, Tokyo.

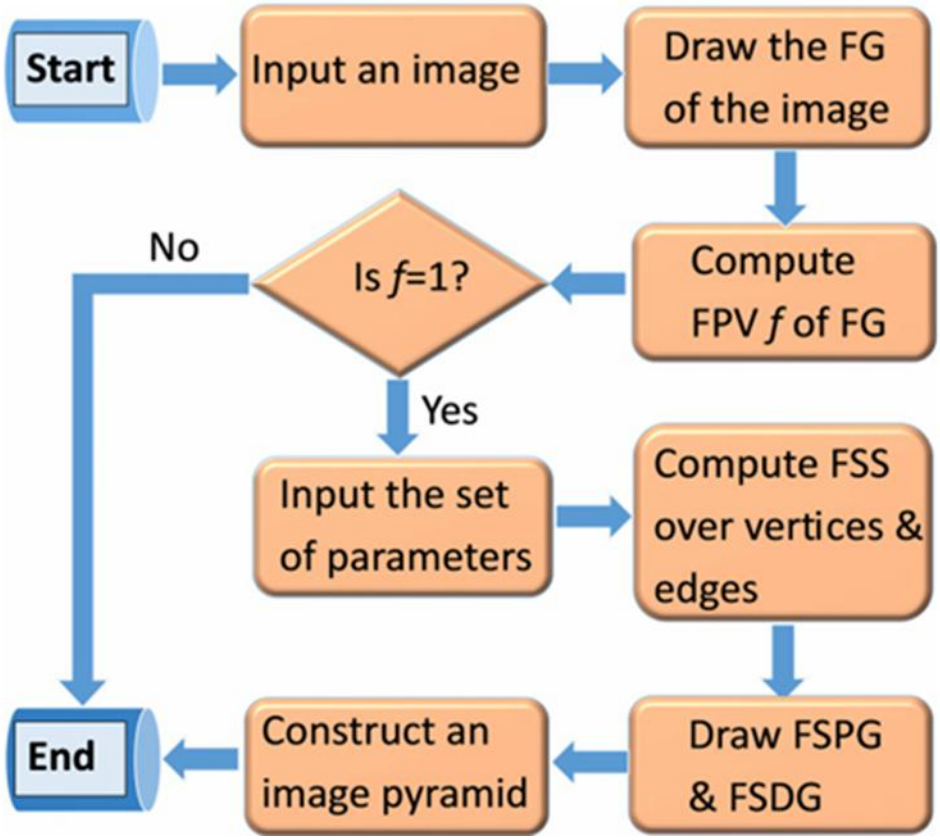

Fig.9. Flowchart of presented Algorithm (2.4)

(2.4) Algorithm:

Step 1**.** Select an image for the contraction**.**

Step 2**.** The colored pixels in the image represent vertices of the FG. To proceed, compute the membership values corresponding to the intensity of each pixel (vertex). Neighboring colored pixels are connected by edges in the

FG. Also, calculate the membership values for edges in the FG. Determine the crossing edges in the FG and compute the fuzzy planarity value for it.

Step3. if $f \neq 1$, then

Stop, else follow step 4

Step4. We apply the fuzzy soft concept for the segmentation of the original image. Choose parameters c_i calculate the FG in a fuzzy soft context.

Step5. Compute FSSs over vertices and edges with respect to the parameters.

Step6. Draw the FSPG $\widehat{H}(c_i)$ for the selected segmented image.

Step7. Determine the fuzzy faces in the FGs corresponding to each parameter.

Step8. Draw the fuzzy dual graphs for each parameter.

Step 9. Finally, construct an image pyramid of the corresponding contracted images based on FSPGs.

The Flowchart of the proposed algorithm is also given in Fig. 4.2.4. Here, we apply the proposed algorithm as follows.

(2.5) [7]. Bipolar fuzzy graphs approach in image shrinking:

(2.5.1) Definition: Let $\mathbb{X}$, be a nonempty set. A bipolar fuzzy set $\mathcal{B}in\ \mathbb{X}$ in is defined as:

$$\mathcal{B} = \{(x, \mu_{\mathcal{B}}^{\mathcal{P}}(x), \mu_{\mathcal{B}}^{\mathcal{N}}(x)) \mid x \in \mathbb{X}\}$$

Here, $\mu_{\mathcal{B}}^{\mathcal{P}}: \mathbb{X} \to [0,1]$ and $\mu_{\mathcal{B}}^{\mathcal{N}}: \mathbb{X} \to [-1,0]$ are mappings. The positive membership degree $\mu_{\mathcal{B}}^{\mathcal{P}}(x)$ represents the degree to which an element x satisfies the property associated with the bipolar fuzzy set $\mathcal{B}$ Conversely, the negative membership degree $\mu_{\mathcal{B}}^{\mathcal{N}}(x)$ represents the degree to which an element

x satisfies some implicit counter property associated with $\mathcal{B}$

If $\mu_{\mathcal{B}}^{\mathcal{P}}(x) \neq 0$ and $\mu_{\mathcal{B}}^{\mathcal{N}}(x) = 0$, it means x only positively satisfies the property of $\mathcal{B}$

If $\mu_{\mathcal{B}}^{\mathcal{P}}(x) = 0$ and $\mu_{\mathcal{B}}^{\mathcal{N}}(x) \neq 0, x$ does not satisfy the property of $\mathcal{B}$ but somewhat satisfies the counter property of $\mathcal{B}$ It is also possible for x to have both $\mu_{\mathcal{B}}^{\mathcal{P}}(x) \neq 0$ and $\mu_{\mathcal{B}}^{\mathcal{N}}(x) \neq 0$ the membership functions of the property and its counter-property overlap in some region of $\mathbb{X}$.

For simplicity, the symbol $\mathcal{B} = (\mu_{\mathcal{B}}^{\mathcal{P}}, \mu_{\mathcal{B}}^{\mathcal{N}})$ will be used to denote the bipolar fuzzy set:

$$\mathcal{B} = \{(x, \mu_{\mathcal{B}}^{\mathcal{P}}(x), \mu_{\mathcal{B}}^{\mathcal{N}}(x)) \mid x \in \mathbb{X}\}$$

(2.5.2) Theorem: A bipolar fuzzy graph ψ is bipolar fuzzy outer planar if and only if it contains no bipolar fuzzy sub graph homomorphic from $K_4 or\ K_{2,3}$.

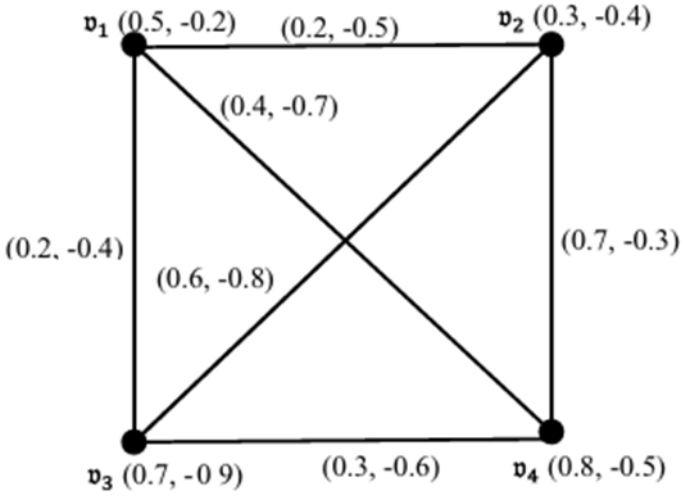

Fig.10. Bipolar fuzzy graph K_4

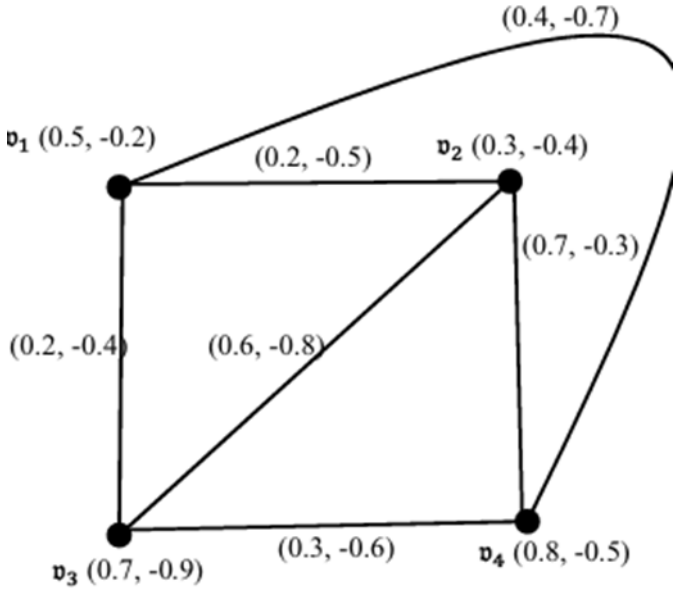

Fig.11. Bipolar Fuzzy planar embedding of K_4

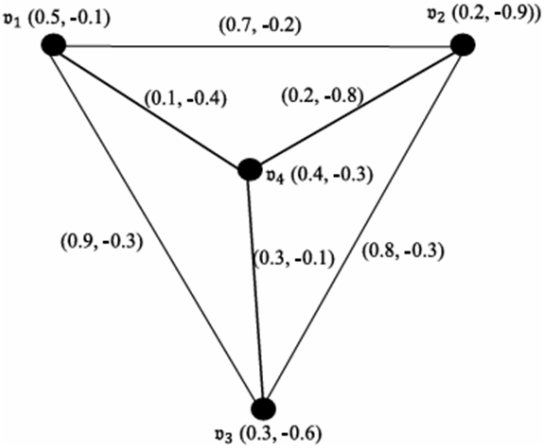

Fig.12. Bipolar fuzzy graph K_4

Proof. It is known that K_4 *or* $K_{2,3}$ are not bipolar fuzzy outerplanar. Thus, no bipolar fuzzy graph having a bipolar fuzzy subgraph homomorphic from $K_4 or K_{2,3}$ is bipolar fuzzy outerplanar graphs shown in the Figs.4.3.3. and 4.3.4.

Conversely, suppose ψ is a bipolar fuzzy graph containing no bipolar fuzzy subgraph homomorphic from $K_4 or K_{2,3}$ By kuratowski's theorem,ψ is planar. Assume G is not bipolar fuzzy outer planar graph. Thus, without loss of generality, we assume that is a cyclic block which is not bipolar fuzzy outerplanar graph. Further we assume that ψ is so embedded in the fuzzy plane that the exterior region contains maximum number of vertices.

The exterior region is bounded by a cycle C. Since not all vertices of ψ , lie on C, there are one or more vertices lying interior to C. If there exist a vertex $\mathfrak{v}_3$

interior on C and three mutually disjoint paths between $\mathfrak{v}_3$ and three distinct vertices of C, then ψ contains fuzzy subgraph homomorphic from K_4. Otherwise, since ψ is a cyclic block, there must exists a vertex $\mathfrak{v}_3$ and two disjoint paths between v3 and two disjoint vertices $\mathfrak{v}_1$ *and* $\mathfrak{v}_5$ on C. Moreover, from the above choice of C, the edge $\mathfrak{v}_1\mathfrak{v}_5$ does not belong to C. This implies ψ contains a bipolar fuzzy subgraph homomorphic from $K_{2,3}$. This is a contradiction. Therefore, Fig.4.3.5. ψ is a bipolar fuzzy outerplanar graph. This completes the proof.

(2.5.3) Definition: Maximum ED- bipolar fuzzy outerplanar subgraph.

If $\psi' = (\mathbb{V}', \tau', \delta')$ with positive and negative size $b' = (b'_{\mathcal{P}}, b'_{\mathcal{N}})$ is the Edge Deletion bipolar fuzzy outerplanar subgraph of non-outerplanar bipolar fuzzy graph $\psi = (\mathbb{V}, \tau, \delta)$ such that there is no other Edge Deletion bipolar fuzzy outerplanar subgraph ψ'' of size , $b'' = (b''_{\mathcal{P}}, b''_{\mathcal{N}})$ of ψ such that $\dot{b}'' > \dot{b}'$, then ψ' is the maximum bipolar fuzzy outerplanar subgraph of ψ.

The following section an application of bipolar fuzzy outerplanar graphs in image shrinking is demonstrated [7].

Image segmentation plays a vital role in dividing digital images into distinct parts or segments, which is essential for recognizing objects within those images. This process is particularly useful in areas such as computer vision and remote sensing. The primary objective of image segmentation is to extract specific objects of interest from the background, allowing for more focused analysis. Different methods can be employed for segmenting images. One such approach involves using Bipolar Fuzzy Outerplanar Graphs to facilitate image shrinking by segmenting various regions of an image. In this context, an image is composed of pixels, which can be grouped into homogeneous sections. Each pixel can be represented as a vertex in a graph, where its membership value either positive or negative is determined by its intensity. Overall, image segmentation serves as a foundational technique in digital image processing, enabling the identification and isolation of relevant features within an image through various methodologies.

Two adjacent pixels (vertices) are connected by edges. The positive membership value (or negative membership value) of an edge is determined by the dissimilarity (or similarity) value of the corresponding pixels (vertices). There are several methods to measure the dissimilarity or similarity between two pixels, and one of these methods is used to determine the edge membership values. Consequently, the entire image (see Fig.14 as an example) is transformed into a Bipolar fuzzy graph (see Fig.15.), where each coloured vertex represents a corresponding segmented coloured section of the image from Fig.14. The edge membership values for the graph shown in Fig.15, are listed in Table.1. Clearly, this graph is a Bipolar fuzzy non outerplanar graph. Moreover, A bipolar fuzzy graph that cannot be embedded in the plane so that each vertex lies on the exterior region's boundary. The Bipolar fuzzy dual graph of this Bipolar fuzzy outerplanar graph can be drawn using the method described (see Fig.16). The face and edge membership values of the Bipolar fuzzy dual graphs shown in Fig.16. are provided in Table4.3.2. Now, we define related terms such as edge shrinking and kernel shrinking. Let $\psi = (A^{\circ}, B)$ represent a bipolar fuzzy graph and consider an edge (a, b) .When this edge is shrunk, a new vertex, denoted as c, is created. This new vertex c will have all the edges that were previously connected to vertices a and b now connected to it, while the edge (a, b) is removed from the graph. The positive membership value for vertex is defined as $\tau^{\mathcal{P}}(\mathfrak{c}) = max\{\tau^{\mathcal{P}}(\mathfrak{a}), \tau^{\mathcal{P}}(\mathfrak{b})\}$ Similarly, the negative membership value for vertex c is given by $\tau^{\mathcal{N}}(\mathfrak{c}) = max\{\tau^{\mathcal{N}}(\mathfrak{a}), \tau^{\mathcal{N}}(\mathfrak{b})\}$.

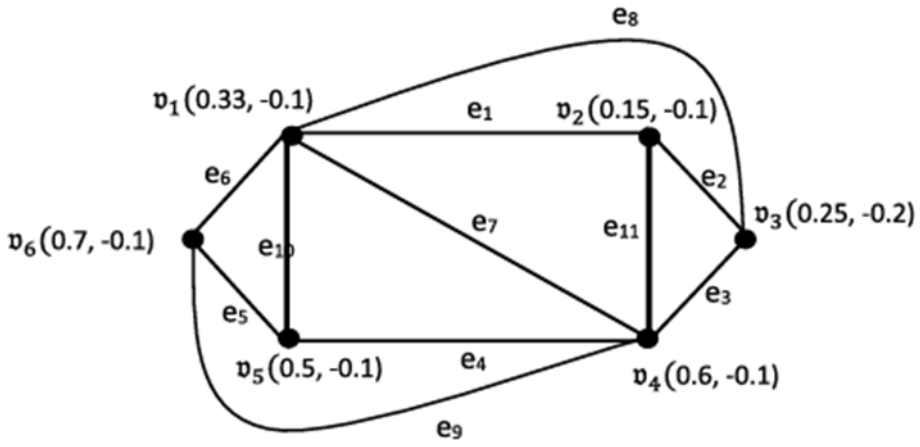

(a)

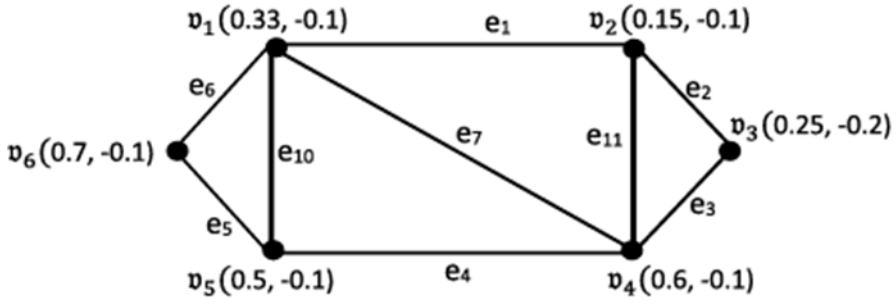

(b)

Fig.13. (a) and (b). Bipolar fuzzy graphs ψ (b). Maximum and maximal Edge Deletion from a bipolar fuzzy subgraph of ψ

Fig.14 An example of color image for image shrinking

When multiple vertices are shrunk simultaneously, an extended shrinking technique known as kernel shrinking is applied. For instance, if the edges $(\mathfrak{v}_2, \mathfrak{v}_6), (\mathfrak{v}_4, \mathfrak{v}_6)$ are to be shrunk at the same time, we denote the vertices involved as $\mathfrak{v}_2, \mathfrak{v}_4$ *and* $\mathfrak{v}_6$ with their respective membership values defined as

$\tau^{\mathcal{P}}(i) = m_i, \tau^{\mathcal{N}}(i) = n_i$ In this case, all these edges are merged into a single vertex, referred to as $\mathfrak{h}$. The positive membership value of vertex $\mathfrak{h}$ is determined max $\{m_i, i = v_2, v_4\}$, while the negative membership value is given by max $\{n_i, i = v_2, v_4\}$. It is important to note that the vertices v_2 *and* $v_4$are combined into the new vertex $\mathfrak{h}$.

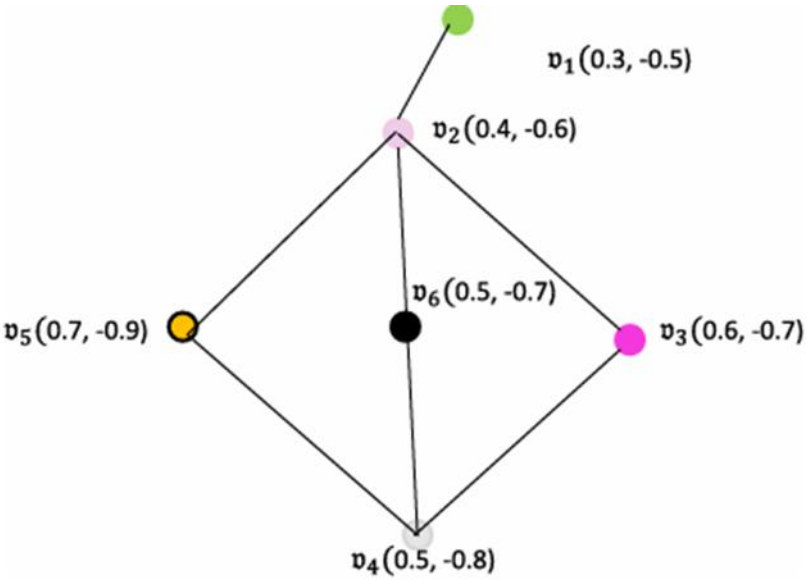

Fig.15. Bipolar fuzzy non-outerplanar graph corresponding to the image

Edge	Membership values
(v_1, v_2)	$(0.2, -0.2)$
(v_2, v_3)	$(0.3, -0.3)$
(v_3, v_4)	$(0.1, -0.1)$
(v_4, v_5)	$(0.4, -0.4)$
(v_2, v_5)	$(0.3, -0.4)$
(v_2, v_6)	$(0.2, -0.3)$
(v_4, v_6)	$(0.4, -0.5)$

Table.1. The edge membership values associated with the edges in the graph shown in Fig.13b.

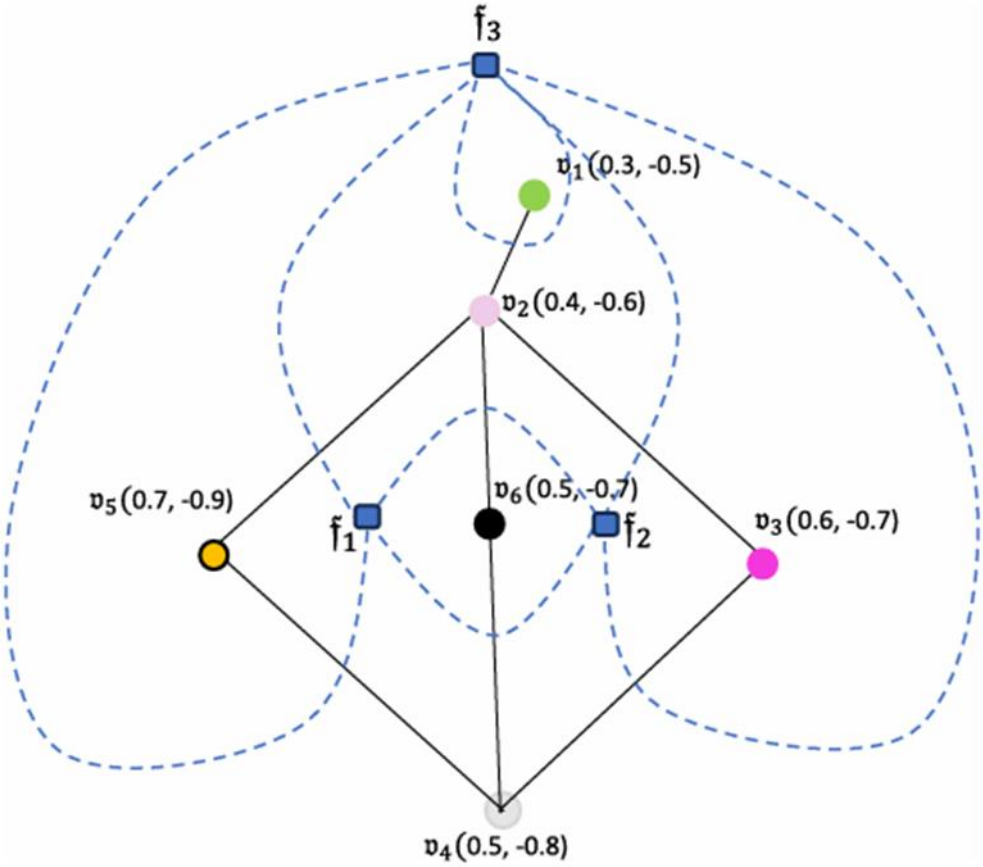

Fig.16. Corresponding Bipolar fuzzy dual graph of the Bipolar fuzzy non outerplanar graph.

A collection of homogeneous pixels constitutes a homogeneous section. Two pixels or two homogeneous sections are considered nearly homogeneous if the difference in their membership values is less than a specified positive threshold. These nearly homogeneous sections undergo a process of shrinking at various levels, with each level derived from the previous one. As illustrated in Fig.15, an image is segmented into distinct regions, each defined by boundaries. In the context of Bipolar fuzzy dual graphs, these edges represent the boundaries of the images.

Consider a bipolar fuzzy non outerplanar graph $\psi = (\mathbb{V}, Å, \mathcal{B})$ as shown in Fig. 16. where

$\mathbb{V} = \{\mathfrak{v}_1, \mathfrak{v}_2, \mathfrak{v}_3, \mathfrak{v}_4, \mathfrak{v}_5, \mathfrak{v}_6\}$,

$$Å = \begin{cases} (\mathfrak{v}_1, (0.3, -0.5)), (\mathfrak{v}_2, (0.4, -0.6)), \\ (\mathfrak{v}_3, (0.6, -0.7)), (\mathfrak{v}_4, (0.5, -0.8)), (\mathfrak{v}_5, (0.7, -0.9)), (\mathfrak{v}_6, (0.5, -0.7))\}, \end{cases}$$

$$\text{and } \mathcal{B} = \{((\mathfrak{v}_1, \mathfrak{v}_2), (0.2, -0.2)), ((\mathfrak{v}_2, \mathfrak{v}_3), (0.3, -0.3), ((\mathfrak{v}_3, \mathfrak{v}_4), ((0.1, -0.1)),$$

$$((\mathfrak{v}_4, \mathfrak{v}_5)), (0.4, -0.4), ((\mathfrak{v}_2, \mathfrak{v}_5), (0.3, -0.4)), ((\mathfrak{v}_2, \mathfrak{v}_6), (0.2, -0.3)),$$

$$(\ (\mathfrak{v}_4, \mathfrak{v}_6), (0.4, -0.5).$$

Faces	Membership values	Edges	Membership values
f_1	$(0.5,-0.5)$	(v_2, v_6)	$(0.2, -0.3)$
		(v_6, v_4)	$(0.4, -0.5)$
		(v_2, v_5)	$(0.3, -0.4)$
		(v_5, v_4)	$(0.4, -0.4)$
f_2	$(0.2, -0.14)$	(v_2, v_6)	$(0.2, -0.3)$
		(v_6, v_4)	$(0.4, -0.5)$
		(v_2, v_3)	$(0.3, -0.3)$
		(v_3, v_4)	$(0.1, -0.1)$
f_3	$(0.2, -0.14)$	(v_2, v_5)	$(0.3, -0.4)$
		(v_4, v_5)	$(0.4, -0.4)$
		(v_2, v_3)	$(0.3, -0.3)$
		(v_3, v_4)	$(0.1, -0.1)$
		(v_1, v_2)	$(0.2, -0.2)$

Table.2. Faces and edge membership values in the bipolar fuzzy dual graph shown in Fig.16.

The bipolar fuzzy non outerplanar graph has the following faces.

i. Bipolar fuzzy face f_1 is bounded by
$\big((v_2, v_6), (0.2, -0.3)\big), \big((v_4, v_6), (0.4, -0.5), \big((v_2, v_5), (0.3, -0.4)\big),$
$\big((v_4, v_5)\big), (0.4, -0.4),$

ii. Bipolar fuzzy face f_2 is bounded by $\big((v_2, v_6), (0.2, -0.3)\big), \big((v_4, v_6), (0.4, -0.5), \big((v_2, v_3), (0.3, -0.3),$
$\big((v_3, v_4), (0.1, -0.1)\big)$

iii. The outer bipolar fuzzy face f_3 is surrounded by $\big((v_2, v_5), (0.3, -0.4)\big), \big((v_4, v_5)\big), (0.4, -0.4),$
$\big((v_2, v_3), (0.3, -0.3), \big((v_3, v_4), (0.1, -0.1)\big), \big((v_1, v_2), (0.2, -0.2)\big).$

The bipolar fuzzy faces f_1 , $f_2 and\ f_3$ are $(0.5, -0.5), (0.2, -0.14)$ and $(0.2, -0.14)$. Then bipolar fuzzy faces as shown in the Fig. 16. Now it's a Bipolar fuzzy outerplanar graph.

In stage 1 of the image pyramid shown in the Fig.17, each pixel is treated as a vertex. Two adjacent pixels or regions that are homogeneous or nearly homogeneous are combined into a single section. This is achieved through edge or kernel shrinking on the Bipolar Fuzzy graph. As part of this process, the corresponding edges in the dual graph are also removed. The resulting shrunk image appears at the top stage of the pyramid. Bipolar fuzzy outerplanar graphs can be effectively utilized in image shrinking processes. By transforming a bipolar fuzzy non-outerplanar graph into a bipolar fuzzy dual graph, it becomes a bipolar fuzzy outerplanar graph. This transformation enables the use of the unique properties of bipolar fuzzy outerplanar graphs to reduce the image size efficiently. This approach maintains essential image features and structures while minimizing storage requirements. The bipolar fuzzy attributes provide a nuanced handling of image data, accounting for various levels of uncertainty and bipolarity in pixel values, resulting in high-quality, compressed images suitable for efficient storage and transmission.

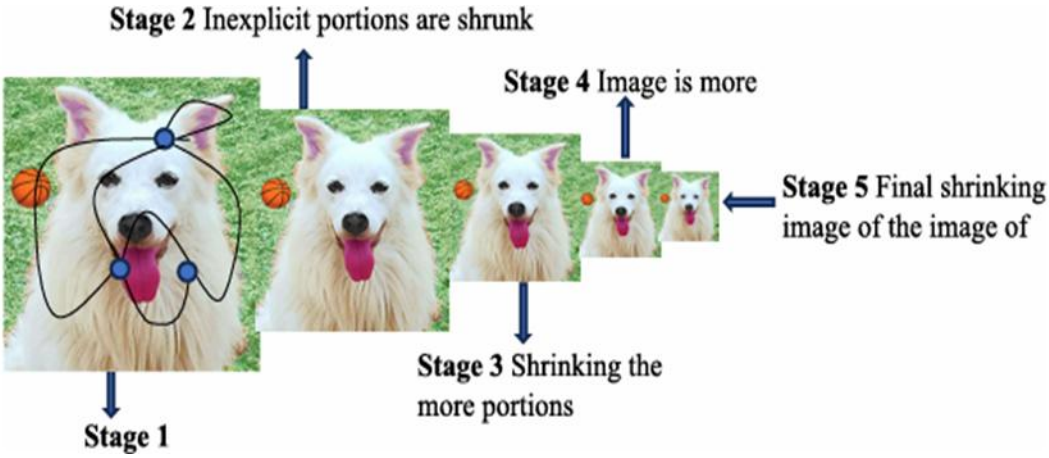

Fig.17. Image Shrinking of the image into image pyramid

III. Conclusion

In this paper, we introduced the concept of bipolar fuzzy outerplanar graphs and explored their various properties and characteristics. We demonstrated how subgraphs of bipolar fuzzy outerplanar graphs can be identified by the strategic removal of vertices or edges. Our analysis included a detailed examination of both maximum and maximal bipolar fuzzy outerplanar subgraphs, considered vertex and edge deletions, and provided illustrative examples to support our findings. Additionally, we delved into the properties of bipolar fuzzy dual graphs, which are closely related to bipolar fuzzy outerplanar graphs, and provided insights into their significance. By expanding the theoretical knowledge and practical utility of bipolar fuzzy outerplanar graphs, this research sets a foundation for continued exploration and innovation in the broader field of fuzzy graph theory. To conclude, we showcased the application of bipolar fuzzy outerplanar graphs in the process of image shrinking. These theories have the potential to enhance algorithms across various domains, including computer vision and image segmentation. The concept can also be expanded to other types of fuzzy graphs, such as interval-valued fuzzy outerplanar graphs and m-polar fuzzy outerplanar graphs. Currently, our focus is on developing interval-valued fuzzy outerplanar graphs.This paper investigates the properties of fuzzy grid graphs and fuzzy ladder graphs, employing machine learning techniques and statistical analysis. Our study reveals strong correlations among these graphs, particularly between: Ladder graphs and fuzzy ladder graphs through machine learning, Grid graphs and fuzzy grid graphs through machine learning. We identify relationships governed by linear and polynomial regression models. Notably, our findings suggest that knowing one index in the crisp case allows for accurate prediction of the corresponding index in the fuzzy case. Key Contributions: 1. Comprehensive analysis of fuzzy grid and ladder graphs. 2. Identification of correlations and predictive relationships using machine learning and statistical methods. 3. Establishment of linear and polynomial regression models connecting crisp and fuzzy graph indices.

References

[1]. Akram, M. Bipolar fuzzy graphs. Inf. Sci. 181(24), 5548–5564.
[2]. Zeeshan Saleem Mufti[1], Hadeel AlQadi[2], Ali Tabraiz[3], Muhammad Farhan Hanif[1], & Mohamed Abubakar Fiidow[4]. Fuzzy and crisp computational analysis of certain graphs structures via machine learning techniques,2025.
[3]. Dinar, J., Hussain, Z., Zaman, S. & Rehman, S. Wiener index for an intuitionistic fuzzy graph and its application in water pipeline network. Ain Shams Eng. J. 14(1), 101826.2022.101826 (2023).
[4]. Wang, W. et al. Low-light image enhancement based on virtual exposure. Signal Process. Image Commun. 118, 117016.2023.
[5]. 7. Gani, A. N., Akram, M. & Subahashini, D. R. Novel properties of fuzzy labeling graphs Hindawi publishing corporation. J. Math. [SPACE]https://doi.org/10.1155/2014/375135 (2014).
[6]. Rosenfeld, A. Fuzzy Graph. In Fuzzy Sets and Their Applications to Cognitive and Decision Process (eds Zadeh, L. A. et al.) 77–95 (Academic press, New York, 1975).
[7]. Deivanai Jaisankar [1], Sujatha Ramalingam [1], Nagarajan Deivanayagampillai [3]& Tadesse Walelign [2], Bipolar fuzzy outerplanar graphs approach in image shrinking,2025.
[8]. Balaraman, G., Sundareswaran, R. & Pal, M. Strong domination integrity in graphs and fuzzy graphs. Intell. Fuzzy Syst. 43(3), 2619–2632 (2022).
[9]. Mahapatra, R., Samanta, S. & Pal, M. Generalized neutrosophic planar graphs and its application. J. Appl. Math Comput. 65, 693–712 (2021).

[10]. Muhiuddin, G., Hameed, S., Rasheed, A. & Ahmad, U. Cubic planar graph and its application to road network. Math. Probl. Eng. 1, 5251627 (2022).
[11]. Ghorai, G. & Pal, M. A study on m-polar fuzzy planar graphs. Int. J. Comput. Sci. Math. 7(3), 283–292 (2016).
[12]. Samanta, S., Pal, M. & Pal, A. New concepts of fuzzy planar graph. Int. J. Adv. Res. Artif. Intell. 3(1), 52–59 (2014).
[13]. Ramya, S. & Lavanya, S. Contraction and domination in fuzzy graphs. TWMS J. Appl. Eng. Math. 13, 133 (2023).
[14]. Mondal, R. & Ghorai, G. Inverse fuzzy mixed planar graphs with application. Int. J. Appl. Comput. Math 10(4), 131 (2024).
[15]. Waheed Ahmad Khan[1,4], Arsh E. Mah Niaz[1,4], Trung Tuan Nguyen[2,4], Minh Hoan Pham[2,4], Thi Minh Ngoc Tong[2,4] & Hai Van Pham[3,4], A fuzzy soft planar graph with application in image segmentation.